International Journal of Research in Engineering, Science and Management
Volume 8, Issue 7, July 2025
https://www.ijresm.com | ISSN (Online): 2581-5792

Geomechanics of Ubaku Field in the Niger Delta using 1-D Mechanical Earth Molding (MEM)

Collins Godswill Ahuchaogu[1*], C. N. Ehirim[2], N. Dagogo[3]
[1]*Student, Department of Physics, University of Port Harcourt, Choba, Rivers State, Nigeria*
[2,3]*University of Port Harcourt, Choba, Rivers State, Nigeria*

Abstract*: This research utilized the Mechanical Earth Modeling approach to evaluate the geo-mechanical properties of the Ubaku field in the Niger Delta for Enhanced Oil Recovery and ensuring maximum resource extraction while minimizing environmental and operational risks. The geo-mechanical properties evaluated include Young's Modulus whose value is between 1.67 to 4.04Mpsi, Poisson's ratio ranges between 0.25 to 0.36, Bulk modulus is between 1.64 to 2.13Mpsi, Shear modulus is between 0.65 and 1.66Mpsi, V_pV_s ratio is between 1.78 to 2.66, S-H$_{min}$ is between 6668.32 to 7722.53psi, S-H$_{max}$ is between 16011.26 to 23991.93psi, overburden stress is between 8805 to 10567.85psiHydrostatic pressure is between 5044.57 to 5112.43psi and fracture pressure lies between 6832.96 to 6930.91psi. With a Young's Modulus indicating moderate stiffness and Poisson's ratio showing mixed brittleness and ductility, the reservoir is suitable for hydraulic fracturing. Stress anisotropy (S-H$_{max}$ vs. S-H$_{min}$) values suggests fractures will propagate along preferred orientations, which must be considered in fracturing design. Variability in shear and Young's modulus highlights zones that may be prone to instability. Proper mud weights and casing designs are essential to mitigate collapse or over-fracturing risks. With overburden stress exceeding horizontal stresses, fractures are likely to propagate horizontally, ensuring containment within the target zone and minimizing caprock breach risks. The reservoir exhibits favorable conditions for operations such as hydraulic fracturing and production, with a mix of brittle and ductile behaviors.

***Keywords*: MEM, V_p/V_s, UCS, AI, YMG SMG, PR, SW, BMG, VSH.**

1. Introduction

When the stress state on a given reservoir is not known and the methods in use does not fully address the solution to the problem, there is every chance that there will be a poor assessment of the reservoir potential. Several International Oil Companies (IOC) have experienced huge losses as a result of poor assessment and the use of obsolete techniques in the course of exploration and Production (Mannon, 2023). When a reservoir begins to experience production decline at an early stage, it is indicative also of an inadequacy in optimal exploration strategy. There is an inherent uncertainty of the stress state in most hydrocarbon reservoirs and there is need to model an approach that will address this uncertainty which will provide better interpretation of the reservoir (Odai and Ogbe, 2010). We adopt the use of geomechanics because it is the scientific study that utilizes both physical formulations and software-driven computations to get a better understanding of how the subsurface rocks deform or fail in response to certain changes such as stress, pressure or other parameters in the environment (www.sciencedirect.com, 2022: www.slb.com, 2016). Reservoir geomechanics provides important reservoir parameters such as; formation porosity, permeability, bottom hole pressures, and wellbore stability. Reservoir geomechanics in the petroleum industry targets to ultimately perform a geo-mechanical evaluation, obtain wellbore stability and optimize hydrocarbon production (Addis, 2017).

2. Materials and Methods

The materials utilized in the course of this work include the following:

(i) The Schlumberger Techlog software; this is used in the entire work in processing the required results of the work. The choice of this software is as a result of its ability to combine the various datasets required to carry out Geo-mechanical characterization of a reservoir.
(ii) Datasets; the data used in this work include Gamma ray logs (GR), Density logs, Sonic logs, resistivity logs, Neutron-porosity logs, Self-Potential (SP) logs, core data, and checkshot data.

The method adopted for this research involves the following:

(i) *First loading the data into the software*: The identified data were loaded successfully into the software. The sequence of events are shown on the flowchart in Fig. 1.
(ii) *QC the data and carry out Well Correlation*: Four wells were studied in the course of this work as shown in Fig. 2. The data QC was done successfully and correlated as shown in Fig. 3.
(iii) *Perform petrophysical evaluation*: Petrophysical evaluation was carried out by means of the required equations as they were loaded into the software, Fig. 3 & 4.

---

*Corresponding author: collins.ahuchaogu@gmail.com

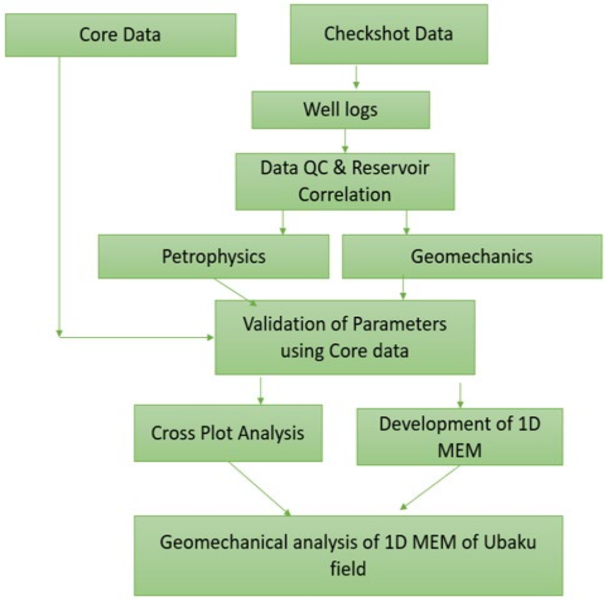

Fig. 1. Work flow

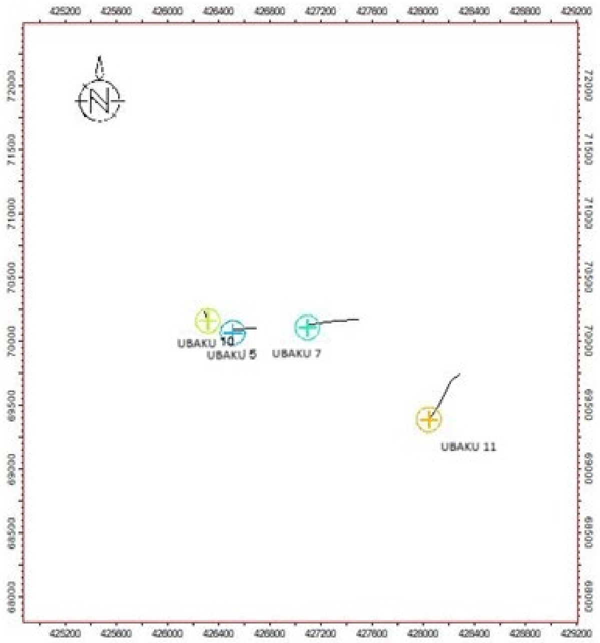

Fig. 2. Well placement

Tota porosity is given by:

$$\phi_t = \phi_{ef} + V_{sh} * \phi_{sf} \qquad (1)$$

Where;

ϕ_t = total porosity of clean sand,
ϕ_{ef} = effective porosity,
V_{sh} = volume of shale in the formation and
ϕ_{sf} = total porosity of shale formation

Water saturation is given by:

$$Sw = \frac{\mathrm{Vp}}{\mathrm{Vw}} \qquad (2)$$

Where;
V_w = Volume of water
V_p = Total pore volume

Also,

$$Sw = \left(\frac{Rw}{R_t} \cdot \frac{1}{\phi^m} \cdot \frac{1}{a}\right)^{\frac{1}{n}} \qquad (3)$$

Where:
ϕ is porosity,
m is the cementation exponent,
a is the tortuosity factor, and
n is the saturation exponent (Archie, 1942).

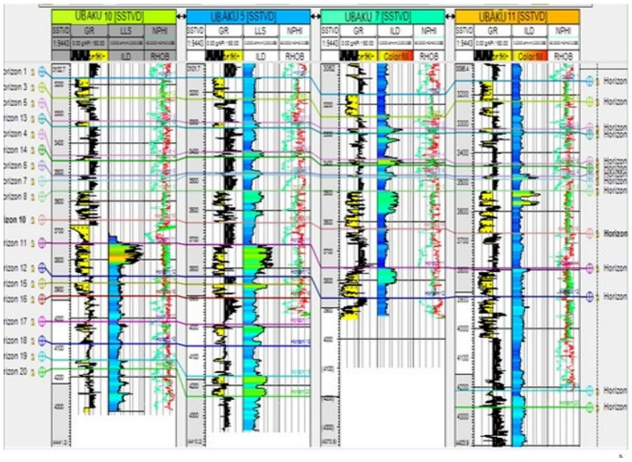

Fig. 3. Well correlation

(iv) *Estimate the geo-mechanical properties*: The geo-mechanical parameters are also estimated by means of the software; the results are shown in table 1 & 2. The following formular help in generating the properties.

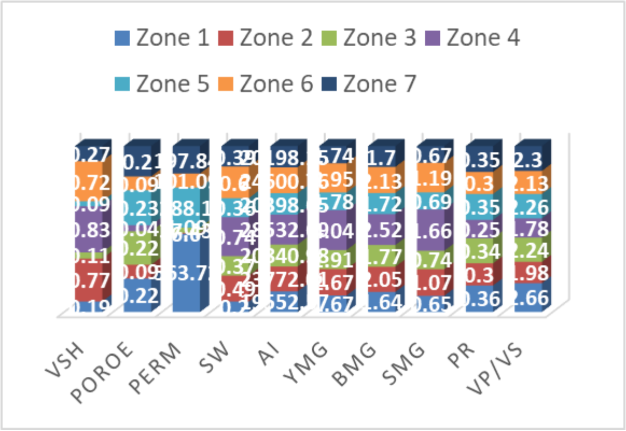

Fig. 4.

Young's modulus: This gives the reservoir's ability to withstand stress denoted as E, describes the relationship between stress (σ) and strain (ε) in a linear elastic material, according to Hooke's Law, hence:

$$E = \frac{\sigma}{\varepsilon} \qquad (4)$$

Bulk modulus: It is a measure of a material's resistance to uniform compression, measured in units Pascal (Pa) or gigapascals (GPa): Mathematically, it is expressed as:

$$K = \frac{-VdV}{dP} \tag{5}$$

where:
K = Bulk modulus
V = Initial volume
dP = Change in pressure
dV = Change in volume

V_p/V_s ratio: This is the ratio of the P-waves velocity to that of the S-wave velocity it is dimensionless. P-wave velocity (V_p) is directly related to the bulk modulus (K) and the density (ρ) of the material:

$$\text{Vp} = \sqrt{\frac{\text{K}+\frac{4}{3}G}{\text{p}}} \tag{6}$$

where G is the shear modulus. Understanding P-wave velocities helps geophysicists interpret subsurface structures and identify hydrocarbon reservoirs (Mavko, Mukerji, & Dvorkin, 2009).

The shear modulus influences the velocity of shear (S) waves traveling through the Earth. S-wave velocity (V_s) is directly related to the shear modulus (G) and the density (ρ) of the material:

$$Vs = \sqrt{\frac{\text{G}}{\rho}} \tag{7}$$

Shear modulus: The shear modulus (G) is defined as the ratio of shear stress (τ) to the shear strain (γ) it produces, hence:

$$G = \frac{\tau}{\gamma} \tag{8}$$

where:
G is the shear modulus,
τ is the shear stress,
γ is the shear strain.

The shear modulus is measured in units of Pascals (Pa) or gigapascals (GPa). It shows how easily or not a material can deform under stress (Schön, 2015).

Unconfined Compressive Strength (UCS): This is defined as the maximum stress a material can endure under uniaxial compression before failing. It is expressed in units of force per unit area, typically megapascals (MPa) or pounds per square inch (psi) (Jaeger, Cook, & Zimmerman, 2007). It can be mathematically represented as:

$$UCS = \frac{F_{max}}{A} \tag{9}$$

Poisson's ratio (ν): This is a fundamental mechanical property that characterizes the elastic behavior of materials, including rocks and soils, under stress. Poisson's ratio (ν) is mathematically expressed as:

$$\nu = \frac{\varepsilon_{lateral}}{\varepsilon_{axial}} \tag{10}$$

where:
$\varepsilon_{\text{lateral}}$ is the lateral strain (perpendicular to the applied stress),
$\varepsilon_{\text{axial}}$ is the axial strain (parallel to the applied stress).

Poisson's ratio typically ranges from 0 to 0.5 for most materials. For geological materials, it generally falls between 0.1 and 0.4, depending on the type of rock or soil and its condition (Jaeger, Cook, & Zimmerman, 2007).

(i) *Validate the results using Core Data:* The core data helps us to match the well data for proper evaluation of the reservoir.
(ii) *Development of 1-D MEM:* This is where the Geo-mechanical properties are evaluated by means of the Techlog interface. The results of this are shown in table 1.
(iii) *Cross Plot Analysis:* This is used to validate the generated geo-mechanical properties: This is done by means of cross plots and charts in the Excel environment; Fig. 1 & Fig. 2.
(iv) *Geo-mechanical Analysis of 1-D MEM:* Here we interpret the results of the Geo-mechanical model generated in terms of the well bore stability, reservoir trajectory, stress analysis and fault regime.

3. Results

The identified reservoir is subdivided into 7 zones for lithology identification the results are shown in table 1 & 2.

Table 1

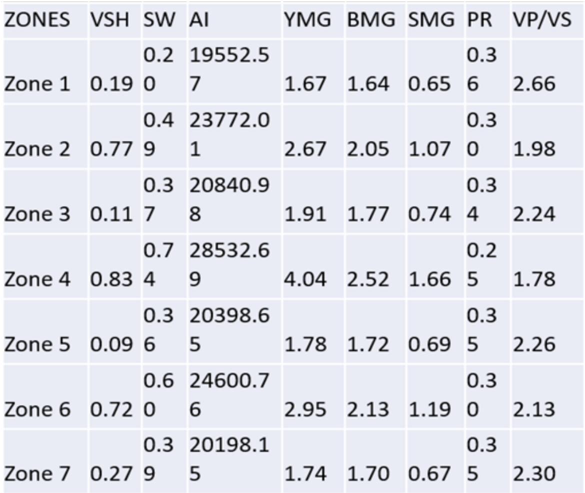

ZONES	VSH	SW	AI	YMG	BMG	SMG	PR	VP/VS
Zone 1	0.19	0.20	19552.57	1.67	1.64	0.65	0.36	2.66
Zone 2	0.77	0.49	23772.01	2.67	2.05	1.07	0.30	1.98
Zone 3	0.11	0.37	20840.98	1.91	1.77	0.74	0.34	2.24
Zone 4	0.83	0.74	28532.69	4.04	2.52	1.66	0.25	1.78
Zone 5	0.09	0.36	20398.65	1.78	1.72	0.69	0.35	2.26
Zone 6	0.72	0.60	24600.76	2.95	2.13	1.19	0.30	2.13
Zone 7	0.27	0.39	20198.15	1.74	1.70	0.67	0.35	2.30

Table 2

Reservoir Zones	Vertical Stress	Pore Pressure	SHMIN	SHMAX	Hydropressure	Fracture Pressure
	psi	psi	psi	psi	psi	psi
Zone 1	10409.73	5256.38	6858.61	21446.06	5044.57	6832.96
Zone 2	10430.37	5265.58	7695.01	16011.26	5053.36	6845.70
Zone 3	8805.00	5276.80	6668.32	23813.29	5064.10	6858.33
Zone 4	10469.67	5283.16	7722.53	16096.51	5070.16	6870.00
Zone 5	10498.83	5296.72	6660.62	23991.93	5083.12	6888.36
Zone 6	10509.71	5301.55	7653.07	16772.54	5087.75	6895.07
Zone 7	10567.85	5325.21	7052.00	21293.52	5112.43	6930.91

4. Discussion

The geo-mechanical properties evaluated include Young's Modulus whose value is between 1.67 to 4.04Mpsi, Poisson's ratio ranges between 0.25 to 0.36, Bulk modulus is between 1.64 to 2.13Mpsi, Shear modulus is between 0.65 and 1.66Mpsi, V_pV_s ratio is between 1.78 to 2.66, S-H_{min} is between 6668.32 to 7722.53psi, S-H_{max} is between 16011.26 to 23991.93psi, overburden stress is between 8805 to 10567.85psiHydrostatic pressure is between 5044.57 to 5112.43psi and fracture pressure lies between 6832.96 to 6930.91psi. The results are shown in Fig. 5 & 6.

A Bulk modulus with a range of 1.64 to 2.93 Mpsi suggests moderate compressibility, which affects pore volume reduction during production. This property is essential for understanding compaction and its effects on reservoir permeability and porosity (Zoback, 2010).

Minimum Horizontal Stress (S-H_{min}: 6668.32–7722.53 psi): This relatively moderate stress indicates regions where the rock may deform without fracturing under certain drilling pressures.

Maximum Horizontal Stress (S-H_{max}: 16011.26–23991.93 psi): These high values suggest a significant anisotropic stress regime, implying the potential for shear failure in specific orientations. Wellbore orientation should align with the direction of minimum stress to minimize instability.

Overburden Stress (8805–10567.85 psi): These pressures reflect the weight of overlying formations and help determine the collapse risk during drilling.

Hydrostatic Pressure (5044.57–5112.43 psi): Consistent values suggest minimal variation in pore pressure, simplifying wellbore pressure management.

Fracture Pressure (6832.96–6930.91 psi): This narrow range defines the upper limit for mud weight. Maintaining mud weight below this pressure is critical to prevent induced fractures (Moos & Zoback, 1990).

V_p/V_s Ratio (1.78–2.66): This range indicates varying lithology. Lower ratios are often associated with brittle rocks, while higher ratios may indicate more ductile or fluid-saturated zones, crucial for fracture and reservoir characterization (Ryder et al., 2018).

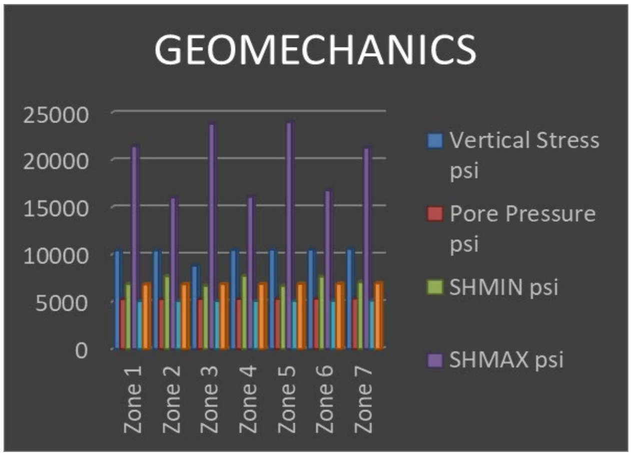

Fig. 5.

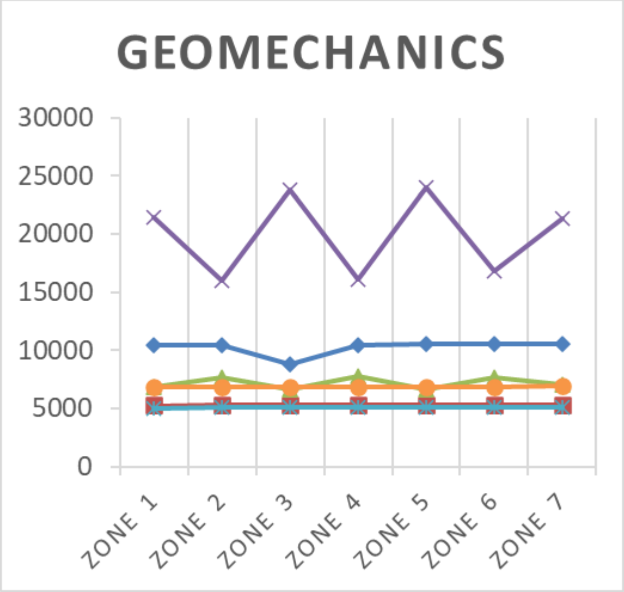

Fig. 6.

5. Conclusion

The reservoir exhibits favorable conditions for operations such as hydraulic fracturing and production, with a mix of brittle and ductile behaviors. With a Young's Modulus indicating moderate stiffness and Poisson's ratio showing mixed brittleness and ductility, the reservoir is suitable for hydraulic fracturing. Stress anisotropy (S-H_{max} vs. S-H_{min}) values suggests fractures will propagate along preferred orientations, which must be considered in fracturing design. Variability in shear and Young's modulus highlights zones that may be prone to instability. Proper mud weights and casing designs are essential to mitigate collapse or over-fracturing risks. With overburden stress exceeding horizontal stresses, fractures are likely to propagate horizontally, ensuring containment within the target zone and minimizing caprock breach risks. Given the stress anisotropy, use hydraulic fracturing along the direction of S-H_{max} to maximize fracture propagation. Select fracturing fluids based on compatibility with the rock's mechanical properties (Economides & Nolte, 2000).

References

[1] Abija, F. A. (2019). Geomechanical Property Evolution and the Mechanics of Growth Faulting in a Niger Delta oilfield, Nigeria. International Journal of Geology & Earth Sciences, pp. 73-95.

[2] Alonso, E. E., Gens, A., & Hight, D. W. (1990). The effect of structure on the shear strength of a natural clay. Geotechnique, 40(3), 405-421.

[3] Ameen, M. S. (2003). Fracture and In-situ stress characterization of hydrocarbon reservoirs. Saudi Arabia: Geological Society Special Publishers.

[4] American Petroleum Institute (API). (2009). Recommended Practice for Drilling Fluids Processing Systems Evaluation (API Recommended Practice 13I). API Publishing Services.

[5] Archie, G. E. (1942). The electrical resistivity log as an aid in determining some reservoir characteristics. Transactions of the AIME, 146(1), 54-62.

[6] Buesser, S., Herrmann, M., & Riedel, W. (2019). Anisotropic mechanical behavior of fiber-reinforced polymers. Journal of Composite Materials, 53(12), 1785-1796.

[7] Bussmann, M. (2017). Single Crystal Materials: Anisotropy, Inhomogeneity, and Interfaces. In Mechanical Behavior of Materials (pp. 281-308). Springer.

[8] Chang, Y., & Bai, B. (2016). Reservoir Rock Properties. In Unconventional Oil and Gas Resources Handbook (pp. 65-97). Elsevier.

[9] Chenevert, M. E., & Sarma, M. S. (1995). Borehole instability—A review. Journal of Petroleum Science and Engineering, 13(4), 245-267.

[10] Coates, G. R., Xiao, L., & Prammer, M. G. (1999). NMR logging: Principles and applications. Halliburton Energy Services.

[11] Dake, L. P. (2001). *Fundamentals of reservoir engineering* (Vol. 8). Elsevier.

[12] Economides, M. J., & Nolte, K. G. (2000). *Reservoir stimulation* (3rd ed.). Wiley.

[13] Economides, M. J., Nolte, K. G., & Valkó, P. P. (2013). Reservoir Stimulation (3rd ed.). Wiley.

[14] Gao, J., Zhang, Y., & Wang, X. (2018). Measurement of dynamic Poisson's ratio using laser Doppler vibrometry. Journal of Sound and Vibration, 433, 115-125.

[15] Gao, X., Zhang, Y., & Chen, Y. (2018). Measurement and prediction of anisotropic mechanical properties of composite materials using finite element method. Journal of Reinforced Plastics and Composites, 37(10), 841-854.

[16] Hubbert, M. K., & Willis, D. G. (1957). Mechanics of hydraulic fracturing. Petroleum Transactions, AIME, 210, 153–168.

[17] Kessey, K. D., & Gray, K. E. (1991). Wellbore instability—Causes and consequences. Journal of Petroleum Technology, 43(9), 1061-1071.

[18] Mannon, R. W. (2023, February 08). Oil Production Forecasting by decline curve Analysis. Retrieved from onepetro.org: http://onepetro.org

[19] Odai L. A. and Ogbe D.D. (2010); Building and Ranking of Geostatistical Petroleum Reservoir Models, M.Sc. Thesis, Unpublished, AUST, December.

[20] Passey, Q. R. (2017). SP log. In Encyclopedia of Petroleum Geoscience (pp. 1-5). Springer.

[21] Peng, X., Li, Z., & Liu, J. (2019). A review on wellbore stability analysis methods for drilling and production operations. Journal of Petroleum Science and Engineering, 172, 107944.

[22] Schlumberger. (1989). *Log interpretation principles/applications*. Schlumberger Wireline & Testing.

[23] Schlumberger. (2018). Oilfield glossary. Retrieved from https://www.glossary.oilfield.slb.com

[24] Schön, J. H. (2015). *Physical properties of rocks: A workbook* (2nd ed.). Elsevier.

[25] Selley, R. C. (1998). Elements of Petroleum Geology (2nd ed.). Academic Press.

[26] Serra, O. (1984). *Fundamentals of well-log interpretation. Volume 1: The acquisition of logging data*. Elsevier.

[27] Short, K. C., & Stauble, A. J. (1967). Outline of geology of Niger Delta. *American Association of Petroleum Geologists Bulletin*, 51(5), 761-779.

[28] Sibson, R. H. (1996). Structural permeability of fluid-driven fault-fracture meshes. Journal of Structural Geology, 18(8), 1031-1042.

[29] Sibson, R. H. (2000). Fault zone models, heat flow, and the depth distribution of earthquakes in the continental crust of the United States. In Continental Scientific Drilling (pp. 101-117). Springer.

[30] Stacher, P. (1995). Present understanding of the Niger Delta hydrocarbon habitat. In M. N. Oti & G. Postma (Eds.), *Geology of Deltas* (pp. 257-267).

[31] Telford, W. M., Geldart, L. P., Sheriff, R. E., & Keys, D. A. (1990). Applied Geophysics. Cambridge University Press.

[32] Terzaghi, K., Peck, R. B., & Mesri, G. (1996). Soil mechanics in engineering practice (3rd ed.). Wiley-Interscience.

[33] Tiab, D., & Donaldson, E. C. (2015). Petrophysics: Theory and practice of measuring reservoir rock and fluid transport properties (4th ed.). Gulf Professional Publishing.

[34] Tiab, D., & Donaldson, E. C. (2019). Petrophysics: Theory and Practice of Measuring Reservoir Rock and Fluid Transport Properties. Gulf Professional Publishing.

[35] Timoshenko, S. P., & Goodier, J. N. (1970). Theory of elasticity. McGraw-Hill.

[36] Vengosh, A., Jackson, R. B., Warner, N., Darrah, T. H., & Kondash, A. (2014). A critical review of the risks to water resources from unconventional shale gas development and hydraulic fracturing in the United States. Environmental Science & Technology, 48(15), 8334-8348.

[37] Wang, H. F., & Nur, A. (1991). Elasticity and seismic anisotropy: A useful framework for rock physics. Geophysics, 56(6), 833–848.

[38] Wang, X., Gao, J., & Zhang, Y. (2017). Dynamic Poisson's ratio measurement using ultrasonic testing. Ultrasonics Symposium (ICU), 2017 IEEE International Conference on Ultrasonics Symposium Proceedings.

[39] Wang, X., Liang, J., & Zhang, Y. (2020). Anisotropic mechanical properties of rocks under complex loading conditions: A review. Rock Mechanics and Rock Engineering, 53(3), 531-543

[40] www.edx.org. (2022, 11 8). Retrieved from reservoir-geomechanics: https://www.edx.org/course/reservoir-geomechanics

[41] Zhang, J. J. (2019). Applied Petroleum Geomechanics. Houston, Texas: Gulf professional publisher.

[42] Zhang, X., & Liu, Z. (2018). Inhomogeneous Materials and Graded Materials. In Mechanics of Materials (pp. 213-239). Springer.

[43] Zhang, Y., Liang, J., & Zhang, Y. (2018). Anisotropic poroelastic behavior of rocks under different loading conditions: A review. Rock Mechanics and Rock Engineering, 51(5), 1455-1470

[44] Zoback, M. D. (2010). *Reservoir geomechanics*. Cambridge University Press.

[45] Zoback, M. D., & Gorelick, S. M. (2012). Earthquake triggering and large-scale geomechanical modeling. Annual Review of Earth and Planetary Sciences, 40, 45–74.

[46] Zoback, M. D. (2019). Reservoir geomechanics: Deformation and failure of reservoir rocks. Cambridge University Press.

[47] Zoback, M. D. (2020). Hydraulic Fracturing in Unconventional Reservoirs: Theoretical and Practical Aspects. Cambridge University Press.

[48] Zoback, M. D. (2007). Reservoir Geomechanics. New York: Cambridge University Press.